INTERNATIONAL JOURNAL FOR NUMERICAL METHODS IN FLUIDS, VOL. 3, 333–345 (1983)

NUMERICAL SIMULATION OF LIQUEFIED FUEL SPILLS: I. INSTANTANEOUS RELEASE INTO A CONFINED AREA

JULIUS BRANDEIS AND EDWARD J. KANSA

Lawrence Livermore National Laboratory, P.O. Box 808, L-451, Livermore, California 94550, U.S.A.

SUMMARY

The shallow-water equations in radial symmetry are solved numerically to simulate the collapse of a cylindrical liquid column into an area surrounded by a concentric dike. The following three subcases of this problem are considered: a liquid column collapsing onto a layer of the same liquid, a liquid column collapsing onto a solid surface, and a column of lighter liquid collapsing onto a heavier liquid (i.e. liquefied natural gas (LNG) spilled onto water). The results for the three categories are compared and the differences and similarities between them are analysed.

KEY WORDS Shallow Water Equations Liquid Column Collapse

INTRODUCTION

The use of liquefied gaseous fuels (LGF) as energy sources is on the increase in the United States. Safe transport and storage of these fuels is very important because of the possible severe consequences of an accidental spill. Lawrence Livermore National Laboratory is investigating the possible consequences of accidental LGF spills for the Department of Energy.

The fuels of interest, such as natural gas, are gaseous at normal ambient temperatures and pressures; however, when condensed into a cryogenic liquid, they are immiscible with water and less dense then water. Consequently, an accidental spill of such a fuel on land or water results in a rapidly spreading liquid pool of evaporating fuel on top of the surface. The liquid fuel vaporizes as it spreads, creating a cold, dense cloud of gaseous fuel. If the vapour cloud is ignited, several different combustion phenomena could occur, such as a pool fire, a flame propagating through the cloud, or an explosion.

In this, the first of two reports dealing with spreading of an LGF, attention is directed to the adaptation and application of the one-dimensional finite difference model[1] for the purpose of simulating an instantaneous release of a liquid from a collapsed storage tank into an area enclosed by a vertical impounding dike.

Three types of such spills are considered, as shown in Figure 1. Together, these represent a set of relevant, though idealized, scenarios for a 'worst-case' accident involving an LGF storage facility. One category includes the cases in which a column of liquid is allowed to collapse onto a body of heavier liquid idealized as having infinite depth. The actual example treated here will be the spill of LNG onto a water surface. Another category deals with the collapse of a liquid column onto a finite depth layer of the same liquid, laying above a solid surface. It will be referred to from this point on, as 'column of liquid collapsing onto a layer of the same liquid'. Finally, the collapse of a liquid column onto a solid surface is considered.

0271–2091/83/040333–13$01.30

Received 4 February 1982
Revised 12 July 1982

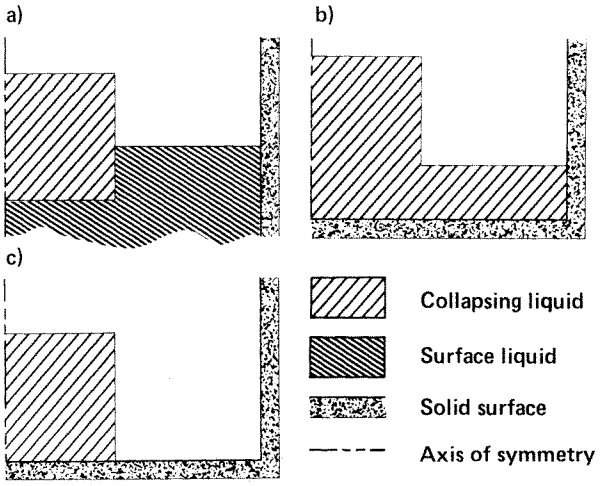

Figure 1. Schematic diagram of the spill geometry: (a) a liquid on a denser liquid, (b) a liquid on a layer of the same liquid, and (c) a liquid on a solid surface

Though similar to the previous case, in that both are bounded from below by a solid surface, this last category is different, since the space between the outer edge of the liquid column and the dike is initially void of any liquid.

The particular class of problems described constitutes a demanding test for any numerical model, since it entails in a single case the collapse of a liquid column, surge against a dike, rebound from the dike and formation of a shock (bore), and its propagation towards the origin. The finite difference approach presented herein is capable of treating all the aspects of the fluid flow without special treatment of shocks. By using a suitably refined grid, and by combining the donor cell differencing scheme with the flux corrected transport (FCT) scheme of Book *et al.*,[2,3] numerical diffusion is kept under control and shock fronts are fairly sharp.

A uniform grid was used for all problems. The number of nodes was increased until there were no noticeable changes in the results. Typically, 60 to 240 grid points, depending on the problem, were needed in order to obtain an error bound of approximately one per cent. The spatial resolution was directly proportional to the scale of the problem.

The subsequent report[4] will focus on the application of the present method to continuous and instantaneous (batch) spills of LNG on an unconfined (undiked) water surface. The emphasis will be directed towards predicting the liquid pool size resulting from very large spills where the volume of the fluid released approaches that of an LNG supertanker compartment (approximately 25,000 m^3).

FORMULATION

The non-linear shallow-water equations with cylindrical symmetry are used to model the spill of a liquid over a surface of a heavier liquid, or over a dry surface. Neglecting viscosity and surface tension, but accounting for evaporation from the LNG surface, the conservation equations for mass and momentum are (cf. References 1 and 6 for the derivation):

$$\frac{\partial(rh)}{\partial t}+\frac{\partial(urh)}{\partial r}+vr=0 \tag{1}$$

$$\frac{\partial u}{\partial t}+\frac{\partial}{\partial r}\left(\frac{u^2}{2}+\delta gh\right)=0 \tag{2}$$

where r and t denote the spatial and the temporal variable, g is the acceleration due to gravity, $h(r, t)$ and $u(r, t)$ are the local height and depth-averaged velocity of the liquid, v is the constant evaporation velocity and $\delta = (1-\rho/\rho_s)$ where ρ is the density of the spilled liquid and ρ_s is the density of the surface liquid. (In spills on a solid surface $\rho_s = \infty$.) Incorporated in equation (2) is the relationship for average hydrostatic pressure, given by

$$p = \tfrac{1}{2}\rho g h \tag{3}$$

Equations (1) and (2) are depth-averaged analogues to conservation laws of mass and momentum and have been successfully used in planar symmetry for similar problems.[5,6] It should be noted that the partial differential equations (1) and (2) are well defined only if $h > 0$.

It will be further assumed that the impounding dike is sufficiently high for no overflow to occur. (Solutions to the shallow-water equations accounting for spillage were given by Greenspan and Young.[5])

In order to fully specify the problem, initial and boundary conditions are formulated. Since the fluid is to be released instantaneously, it is assumed that for $t \leq 0$, the liquid is at rest, and is cylindrical in shape (Figure 1) so that

$$h(r, 0) = h_0 \text{ (or any prescribed distribution)}, \quad u(r, 0) = 0 \quad \text{for } 0 \leq r \leq R_0 \tag{4}$$

$$h(r, 0) = 0 \text{ (or any prescribed distribution)}, \quad u(r, 0) = 0 \quad \text{for } R_0 < r \leq R_w \tag{5}$$

where R_w refers to the location of the dike (wall).

At the axis of symmetry and at the impounding dike the liquid must have zero momentum in the axial direction. Therefore,

$$u(0, t) = 0 \tag{6}$$

and

$$u(R_w, t) = 0 \tag{7}$$

constitute the boundary conditions. The values for the thickness of the liquid at the origin and at the dike must be locally computed from the compatibility equations, using the boundary conditions in equations (6) and (7). Taking advantage of the hyperbolic nature of equations (1) and (2), these compatibility conditions, written in the form of appropriate characteristic equations, are (cf. Appendix)

$$h\frac{du}{dt} - c\frac{dh}{dt} = -cv \quad \text{at} \quad r = 0, \quad \text{along} \quad \frac{dr}{dt} = u - c \tag{8}$$

$$h\frac{du}{dt} + c\frac{dh}{dt} = -c\frac{uh}{r} - cv \quad \text{for} \quad r > 0 \quad \text{and at} \quad r = R_w, \quad \text{along} \quad \frac{dr}{dt} = u + c \tag{9}$$

In equations (8) and (9), c denotes the local speed of propagation of disturbances

$$c(r, t) = \sqrt{[\delta g h(r, t)]} \tag{10}$$

The boundary conditions on u (equations (6) and (7)) have now been specified at the two physical extremities of the computational domain, and h is determined from equations (8) and (9). Together, these are sufficient to close the formulation in all three cases, providing that $h > 0$ everywhere. If this latter criterion is not fulfilled, a boundary condition must be specified at the leading edge of the surge.

Looking first at the collapse of the liquid column onto a layer of the same liquid (with $\delta = 1$), no special problem arises as the liquid layer extends throughout the computational domain. Equations (6)–(9) are sufficient to complete the formulation of the problem.

The cases of a spill on a solid surface ($\delta = 1$) and of a spill of a lighter liquid on a heavier surface liquid ($\delta < 1$) require special treatment whenever $h(r, t) = 0$. Because the partial differential equations are defined only for those regions of space where h is non-zero, appropriate numerical treatment of the leading edge boundary conditions is required whenever the subject liquid propagates into regions devoid of that liquid.

For spills on a solid surface, the velocity was specified at the leading edge by means of an analytic expression. This point will be discussed further in the next section. For spills of a lighter liquid on a heavier liquid, it is assumed that the lighter liquid propagates into the heavier fluid at the same rate as if their densities were equal, which is equivalent to specifying $u = 0$ ahead of the leading edge.

METHOD OF SOLUTION

One frequently used and natural approach to solving the hyperbolic shallow-water equation is the method of characteristics. Although this method avoids many of the numerical problems associated with finite difference methods, its use becomes exceedingly complicated when applied to multiple interacting shock waves in an Eulerian frame. For this reason, a finite difference approach which smears out the discontinuity by a controlled amount of diffusion was preferred for the solution to the flow problem. The amount of numerical diffusion was controlled by combining diffusive donor cell differencing scheme with the FCT scheme.[2,3]

Using the fully explicit second upwind difference scheme (donor-cell) on the terms involving u and central differences on the gravity term, the finite difference analogues to the governing conservation equations are:

$$H_i^{n+1} = H_i^n - \frac{\Delta t}{\Delta r}(U_R \alpha_R - U_L \alpha_L) + \Delta t \Gamma \tag{11}$$

$$U_i^{n+1} = U_i^n - \frac{\Delta t}{\Delta r}(\tfrac{1}{2} U_R \beta_R - \tfrac{1}{2} U_L \beta_L) - \delta g \frac{\Delta t}{2\Delta r}(h_{i+1}^n - h_{i-1}^n) \tag{12}$$

where i and n are, respectively, the spatial and temporal indices, and

$$H_i^n = r_i h_i^n$$
$$U_R = \tfrac{1}{2}(u_{i+1}^n + u_i^n)$$
$$U_L = \tfrac{1}{2}(u_i^n + u_{i-1}^n)$$

and

$$\alpha_R = \begin{cases} H_i^n & \text{if } U_R \geq 0 \\ H_{i+1}^n & \text{if } U_R < 0 \end{cases} \qquad \beta_R = \begin{cases} u_i^n & \text{if } U_R \geq 0 \\ u_{i+1}^n & \text{if } U_R < 0 \end{cases}$$

$$\alpha_L = \begin{cases} H_{i-1}^n & \text{if } U_L \geq 0 \\ H_i^n & \text{if } U_L < 0 \end{cases} \qquad \beta_L = \begin{cases} u_{i-1}^n & \text{if } U_L \geq 0 \\ u_i^n & \text{if } U_L < 0 \end{cases}$$

The evaporation term is defined as $\Gamma = -v r_{i-1}$.

The compatibility conditions in equations (8) and (9) are discretized along the appropriate characteristic (see Figure 2) and use is made of the boundary conditions in equations (6) and

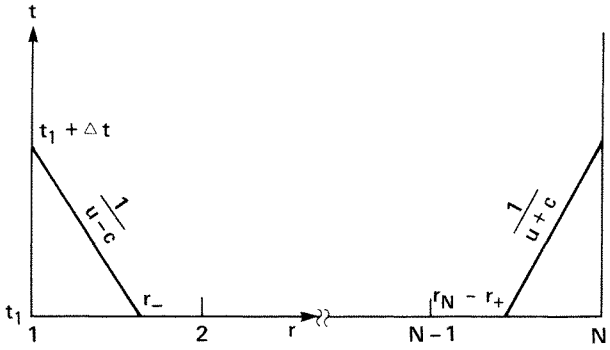

Figure 2. Schematic diagram for computing the boundary conditions using r–t space: (a) at the origin, (b) at the leading edge and at the wall

(7), to give the following finite difference analogues

$$h_1^{n+1} = h_+^n \frac{(u_+^n/2 - c_+^n)}{(-u_+^n/2 - c_+^n)} - \frac{c_+^n v r_+ \Delta t}{(-u_+^n/2 - c_+^n)} \tag{13}$$

$$h_w^{n+1} = h_-^n \frac{(u_-^n/2 + c_-^n)}{(-u_-^n/2 + c_-^n)} - \frac{(c_-^n u_w^n h_w^n + c_-^n v r_w)\,\Delta t}{r_w(-u_-^n/2 + c_-^n)} \tag{14}$$

where the symbols + and − denote the values of the variables at the left-running and right-running characteristics, interpolated at the previous time step.

For completeness it is noted that an alternative, simpler method was successfully tried in place of the compatibility relation at the wall (equation (14)). That approach sets h_w according to the amount of mass needed at the finite difference cell adjacent to the wall in order to conserve the total mass within the system. Since this method tends to mask any possible numerical errors, the characteristics approach (equation (14)) was preferred.

The numerical formulation of the leading edge velocity criterion for spills on a solid surface, based on the characteristics approach (equation (9)), presented a special problem due to the existence there of a very thin layer of liquid tangent to the surface. As an alternative, the velocity of the leading edge was assigned to be $2\sqrt{(gh_0)}$. This analytical result for spills with planar symmetry[5] is the maximum velocity possible for the flow. (In the present axisymmetric case the actual leading edge velocity will be smaller.) Numerical experimentation has shown the computed results to be insensitive to the value of the assigned leading edge velocity as long as it exceeds the actual flow velocity. For these cases, a region of zero thickness (no mass) was formed between the actual and the assigned edge.

The stability conditions for the finite difference equations (11) and (12) is given by Hibberd and Peregrine.[6]

$$\frac{\Delta t}{\Delta x} < \frac{1}{|u_{MAX}| + c_{MAX}} \tag{15}$$

The present method is simpler than the Lax–Wendroff scheme used by Hibberd and Peregrine[6] to solve the shallow-water equations, while still retaining the conservative and advective difference form, as well as the ability to treat shocks and reflections of fluid from obstacles.

As in Reference 6, parasitic numerical oscillations were encountered in the solutions. These were successfully eliminated to the degree desired, by the use of an FCT algorithm

described by Book *et al.*[2] and Boris and Book.[3] This technique first diffuses the variable being processed, then flux-corrects it, and finally carries out anti-diffusion, while maintaining the conservative property of the equations.

The effects of destabilizing truncation errors associated with the finite difference scheme were analysed using appropriate second-order accurate expressions for both time and space derivatives. The results showed no significant influence of these terms because both sufficiently fine grid spacing and the donor cell differencing scheme combined with FCT were used.

NUMERICAL RESULTS AND DISCUSSION

The method described in the previous sections has been used to simulate the various categories of instantaneous spills into an area enclosed by a dike. A good portion of the results presented are for cases whose geometry and dimensions were chosen to allow comparison with available experimental and computational results. Most often these studies employ water as both the spilled and the surface liquid. However, since the density appears in the governing equations only as the ratio of the spilled liquid density to the surface density, these results have a broader validity. In cases where comparisons of different sets of results are made, an attempt was made to keep constant the mesh size as well as all other parameters influencing the numerics.

Figure 3 presents a comparison of solutions obtained for a collapse of a cylindrical column of liquid on: (a) a solid surface, (b) a layer of the same liquid, and (c) a liquid of higher density (this case simulates an LNG spill on water where δ was 0·55 [for the density ratio ρ_{LNG}/ρ_{WATER} of 0·45] and v was taken as $4{\cdot}23\times10^{-4}$ m/s). For each of the three categories a sequence of plots is presented showing the instantaneous thickness contour of the spilled liquid. It is to be recalled that in the case of two liquids of unequal densities, the lighter liquid is partially submerged in the heavier liquid where the fraction of its height submerged is proportional to the density ratio. The plotted results, therefore, show the second fluid's thickness, and not the height above the undisturbed surface.

Each of the sequences exhibits the essential features of the flow, all observed and photographed in Reference 7. These are: the initial shape of the liquid column, the outward surge following release, impact at the dike, reflected bore traveling towards the origin, and spike produced by the liquid converging at the origin. The described sequence of events repeats itself since the fluid is idealized to be inviscid. The number of such cycles is limited in a real fluid by viscosity, whereas in the numerical simulation the dissipative effects of the residual numerical diffusion will eventually stop all motion.

The significant and well documented[8] difference between a solid surface spill (case a), and the liquid's collapse on liquid (cases b and c), is the formation of a shock front during the initial surge in the latter and its absence in the former. Instead of forming a shock, the free surface of the liquid flowing over the solid surface smoothly slopes to merge tangentially with that surface.

Upon impact on the face of the dike, a thin column of fluid was formed adjacent to the wall for all three cases simulated. In the case of the solid surface spill, this layer reached the highest level of the three cases. At its maximum, this height exceeded the original level of fluid prior to the release. Though the present result is consistent with the findings of Reference 5 (in which special treatment was used), it must be regarded with some scepticism as the assumptions inherent in the model may be violated when high and narrow layers of water form. It is interesting to contrast these results to the present guidelines on the height of

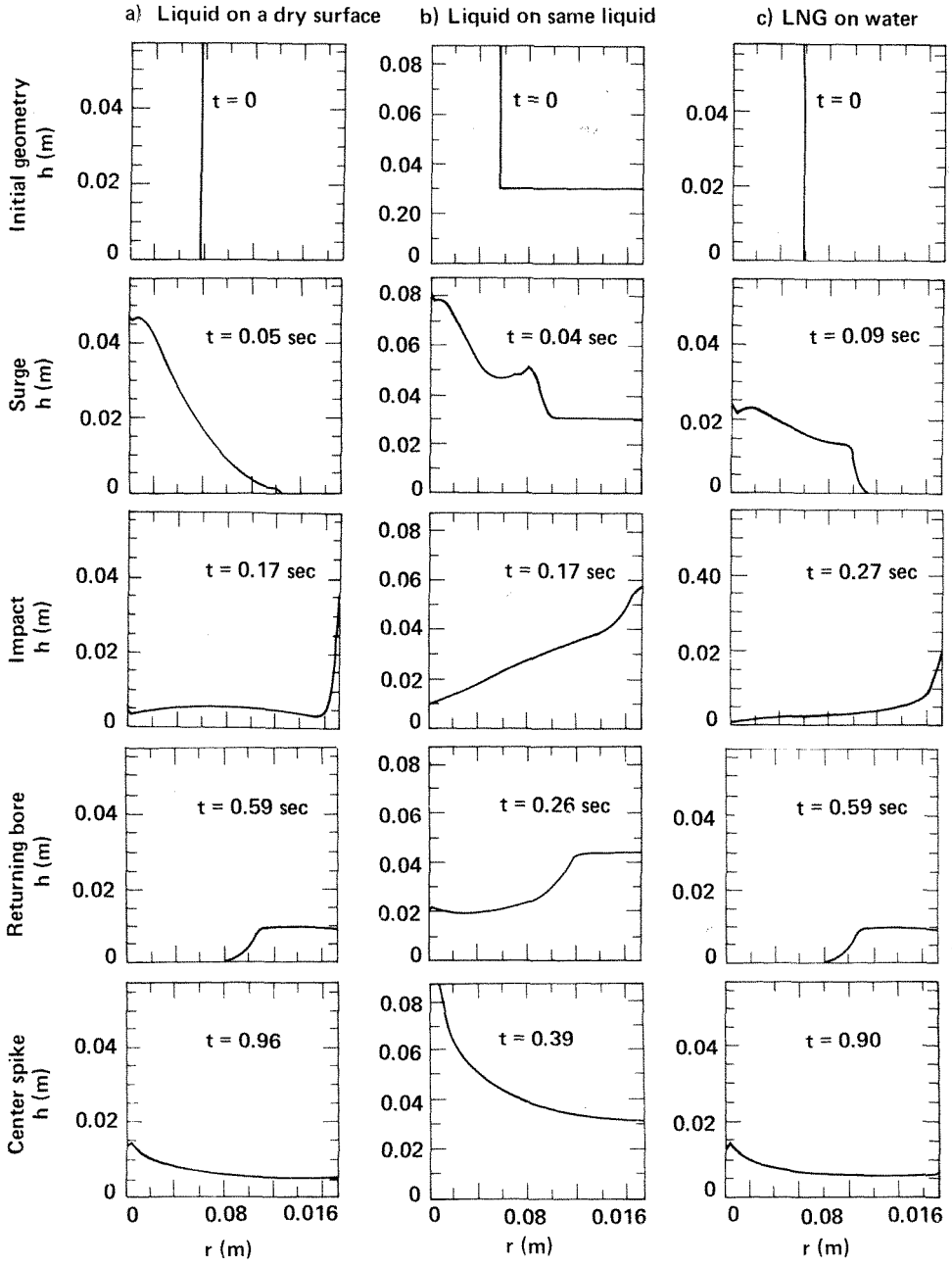

Figure 3. Characteristic sequence over one cycle for the three categories of a liquid column collapsing into an impounded area. (Note the discrepant thickness scale in the set of results: liquid on same liquid)

the impounding wall[9] which requires only that

$$R_w - R_0 \geq h_0 - h_w \tag{16}$$

where R_w and h_w are the location and height of the dike and R_0 and h_0 are the location of the tank's outer wall and the height of the stored liquid. After reflection from the dike has taken place, all three simulations show a bore moving towards the origin into the advancing layer of liquid.

A diagram showing the location as a function of time of the advancing front and the returning bore for the three cases discussed, appears in Figure 4. LNG spilled on water

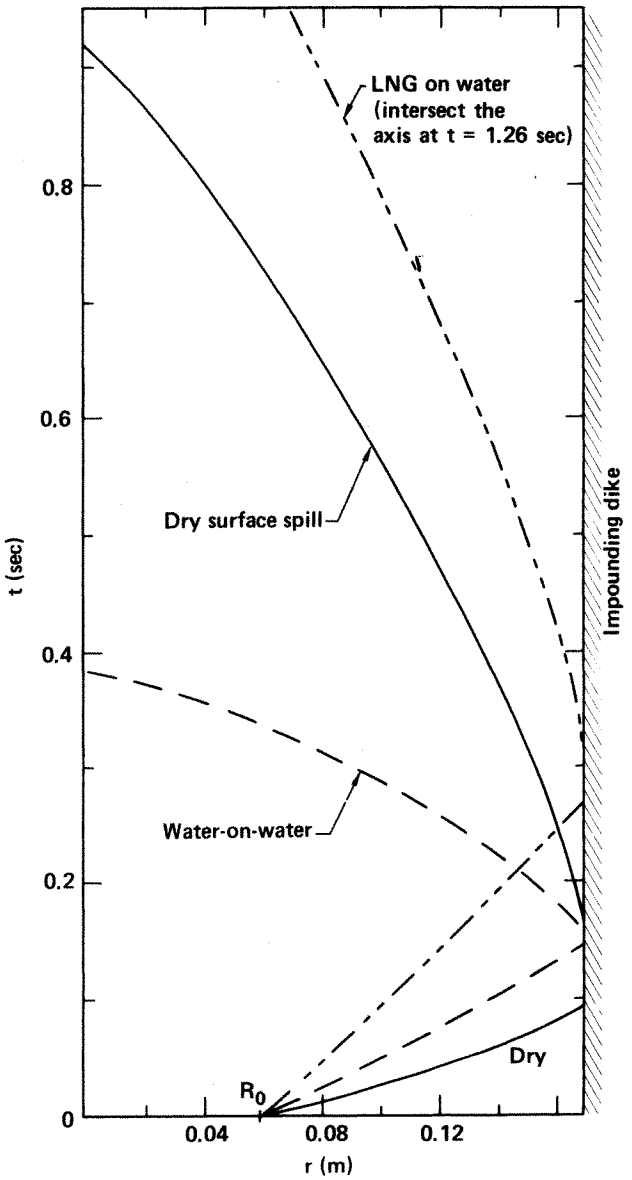

Figure 4. r–t diagram tracing the location of the leading edge of the surge and the returning bore for the three spill categories

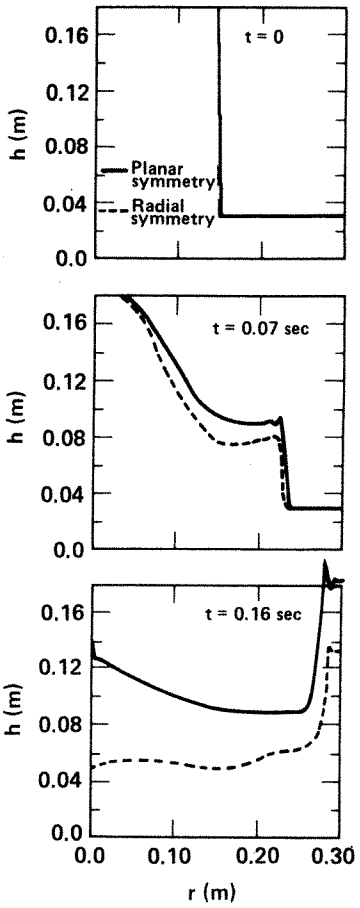

Figure 5. Comparison of the planar and the axisymmetric cases of a liquid column collapsing into the same liquid

shows the slowest spreading rate since it is partially submerged. The solid surface spill spreads at the fastest rate, approaching the limiting value (for the planar symmetry) of $u = 2\sqrt{(gh_0)}$. This fact, together with the slender and uniform thickness distribution noted from Figure 3, accounts for the high and thin layer formed at the dike by impacting fluid. Liquid collapsing onto a layer of the same liquid has an intermediate leading edge velocity which is a function of the depth distribution.

A similar comparitive discussion of the bore returning towards the origin is quite a bit more complicated, as the entire area enclosed by the dike contains fluid flowing in both directions with non-uniform thickness and velocity distributions.

Figure 5 presents a comparison between one-dimensional planar and axisymmetric simulation of a rectangular column of water collapsing into a layer of quiescent water, surrounded by an impounding dike. The particular dimensions used for this problem were chosen to correspond with the example in Reference 8 in which both the experimental and two-dimensional, computational results for the planar cases are given. Since the restraining wall is situated only twice as far from the origin as the boundary initially separating the deep from the shallow water, it is not surprising that for both the advancing and the reflected bore, the planar shock-front leads the radial shock front by only a small amount. There is a noticeable

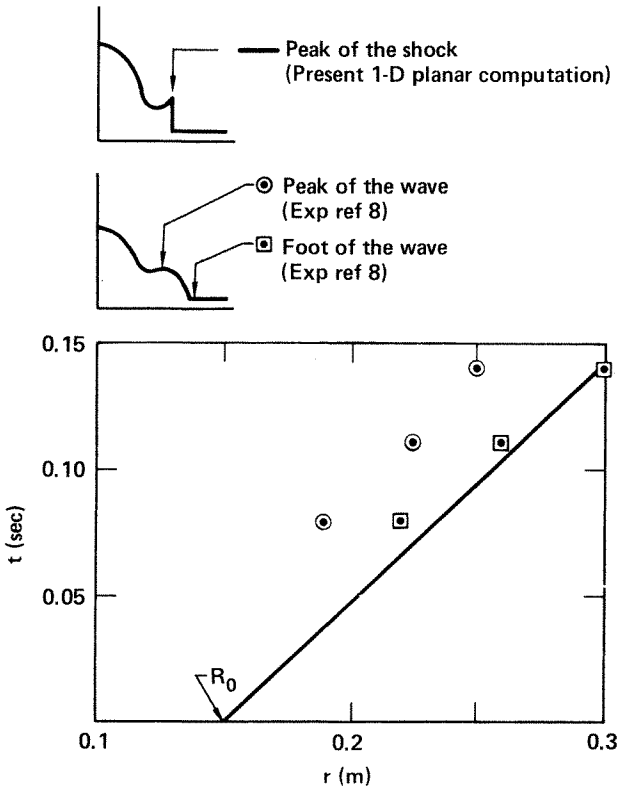

Figure 6. Comparison between experimental results and the computed results using the present method for the collapse of a plane rectangular water column into water

difference in the water height difference across the bore for the two cases as the consequence of mass conservation. These general observations hold for spills of various magnitudes, whether on a liquid surface or on dry land (in the latter case there is no bore prior to reflection from the dike, but the observations on velocity hold for the leading edge of the advancing fluid).

The above results are in fair agreement with those of Reference 8. (See Figure 6). Since the one-dimensional theory converts the potential energy into motion in the radial direction only, it is easy to see why the leading edge velocity is overpredicted by the present method. The present method idealizes the advancing front as a sharp discontinuity while the experiment and the two-dimensional computed results (possible due to poor numerical resolution) show a much more diffused front. For this reason the location of both the peak and the foot of the wave from Reference 8 are shown in Figure 6.

Next, the numerical results obtained by the present method are compared with the experimental results of Martin and Moyce[10] in Figure 7. The fluid used was water and the spill was carried out over a solid surface. The geometry of the column in both the experiment and the simulation prior to instantaneous release was taken as right circular cylinder with the height and radius of 5·72 cm. The results appear to be in fair agreement when the rates of spreading of the liquid are compared. It is interesting to note that Hirt and Nichols[11] showed very good agreement between their two-dimensional Navier–Stokes solution and the experimental results of Reference 10 for the 'broken dam' problem. It should be remembered that

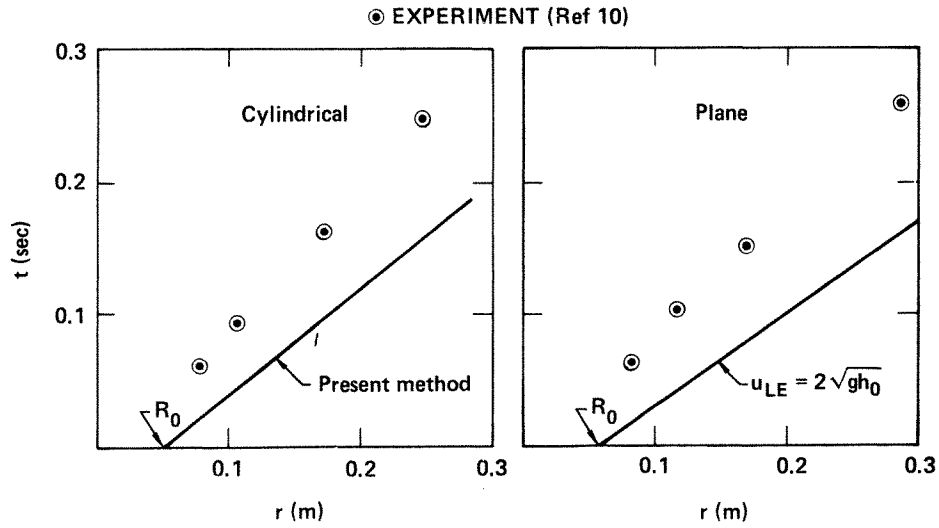

Figure 7. r–t diagram tracing the location of the leading edge of a collapsing column of water, comparing experimental results with results obtained analytically: (a) cylindrical symmetry; (b) planar symmetry

an idealized model was used for the present computation, in which viscosity and surface tension were neglected. These account for at least part of the discrepancy observed. Furthermore, the relative importance of friction and surface tension may be expected to be inversely proportional to the spill size. Therefore, the idealizations used in the model should present less of a hindrance for a larger, more practical spill, at which the present method is aimed.

No attempt was made to resolve the displacement error between the two sets of results. This error is attributable to the experimental difficulties inherent in achieving an instantaneous release as well as in the method of normalization used for reducing the experimental data.

As a further check, a similar comparison is presented in Figure 7 for the planar configuration having the same dimensions and under the same conditions as the case just discussed. Here, the velocity of the leading edge was computed from the well known[5,10] analytical result $u_{LE} = 2\sqrt{(gh_0)}$.

The ratio of the approximate slopes of experimental and calculated results is found to be 1·3 for the cylindrical case, and 1·4 for the planar case. This similarity lends further support to the computed results and the method presented herein.

CONCLUSION

The shallow-water equations in radial symmetry were solved numerically to simulate several possible situations resulting from a hypothetical collapse of a storage tank surrounded by an impounding dike. The model sucessfully dealt with such a collapse using various combinations of liquids and spill conditions. Using no sub-modelling, all the features observed in experiments were numerically simulated. The numerical results were in good agreement with the available experiments, considering the approximate nature of the method.

Comparisons were presented for the following three categories of spills into a diked area: liquid onto a layer of the same liquid, liquid onto a solid surface, and LNG onto water. LNG spilled onto water (i.e. lighter liquid on denser liquid), showed the slowest spreading rate.

The results corroborate the conclusion of Reference 7 that the present height requirements of the impounding dike are insufficient in order to contain totally, a worst-case dynamic spill, especially on a solid surface.

ACKNOWLEDGEMENTS

The authors are grateful to Dr. D. L. Ermak for his many helpful suggestions in the course of this work.

Work performed under the auspices of the U.S. Department of Energy by the Lawrence Livermore National Laboratory under contract number W-7405-ENG-48.

APPENDIX

The method of characteristics seeks a Galilean transformation, dr/dt, having the property that suitable linear combinations of the partial differential equations are exact differentials of time.

In the moving reference frame, the partial differential equations are:

$$\frac{\partial h}{\partial t}+\left(u-\frac{dr}{dt}\right)\frac{\partial h}{\partial r}+h\frac{\partial u}{\partial r}=-\left(v+\frac{uh}{r}\right) \tag{17}$$

$$\frac{\partial u}{\partial t}+\delta g\frac{\partial h}{\partial r}+\left(u-\frac{dr}{dt}\right)\frac{\partial u}{\partial r}=0 \tag{18}$$

Consider two parameters α and β. After equation (17) is multiplied by α, and equation (18) by β, the two expressions are added together. Now it is required that the resulting equation be an exact differential equation of time. Because the resulting coefficients of $\frac{\partial h}{\partial r}$ and $\frac{\partial u}{\partial r}$ must simultaneously vanish, one has

$$\alpha\left(u-\frac{dr}{dt}\right)+\beta\delta g=0 \tag{19}$$

$$\alpha h+\beta\left(u-\frac{dr}{dt}\right)=0 \tag{20}$$

This is satisfied if

$$\frac{dr}{dt} = u \pm c \tag{21}$$

$$\alpha = \pm \frac{c}{h} \tag{22}$$

$$\beta = 1 \tag{23}$$

where

$$c = \sqrt{(\delta g h)} \tag{24}$$

For $r \neq 0$ this results in

$$\pm c\, dh + h\, du = \mp c\left(v + \frac{uh}{r}\right) dt \quad \text{along} \quad \frac{dr}{dt} = U \pm c \tag{25}$$

For $r = 0$, L'Hôpital's rule is applied to equation (18) and a similar procedure is followed.

REFERENCES

1. D. L. Ermak and W. Stein, 'One-dimensional numerical fluid dynamics model of the spreading of liquefied gaseous fuels (LGF) on water', Lawrence Livermore National Laboratory, *UCRL-53078*, November 1980.
2. D. L. Book, J. P. Boris, and K. Hain, 'Flux-corrected transport II: generalizations of the method', *J. Comp Phys.*, **18,** 248–283 (1975).
3. J. P. Boris and D. L. Book, Flux corrected transport III: minimal-error FCT algorithms', *J. Comp. Phys.*, **20,** 397–431 (1976).
4. J. Brandeis and D. L. Ermak, 'Numerical simulation of liquified fuel spills: II. Instantaneous and continuous LNG spills on an unconfined water surface', Lawrence Livermore National Laboratory, Livermore, CA, *UCRL-87205-2*, February 1982. (second paper of the series).
5. H. P. Greenspan, and R. E. Young, 'Flow over a confinement dike', *J. Fluid Mech.*, **87,** Part 1, 179–192 (1978).
6. S. Hibberd and D. H. Peregrine, 'Surf and run-up on a beach, a uniform bore', *J. Fluid Mech.*, **95,** part 2, 323–345 (1979).
7. H. P. Greenspan and A. V. Johansson, 'An experimental study of flow over an impounding dike', *Studies in Appl. Math.*, **64,** 211–223 (1981).
8. C. L. Chenier, M. N. Esmail, G. A. Hill and C. L. Shoole, 'Numerical and experimental study of a falling liquid column', *Canadian J. Chem. Eng.*, **58,** 3–11 (1980).
9. National Fire Protection Association, Inc., 'Storage and handling of liquefied natural gas', *ANSI/NFPA 59A*, (1980).
10. J. C. Martin and W. J. Moyce, 'An experimental study of the collapse of liquid columns on a rigid horizontal plane, part IV', *Phil. Transactions, Royal Society of London*, Series A, **244,** 312–324 (1951–1952).
11. C. W. Hirt and B. D. Nichols, 'Volume of fluid (VOF) method for the dynamics of free boundaries', *J. Comp. Phys.*, **39,** 201–225 (1981).